GEOLOGICA CARPATHICA, DECEMBER 2006, 57, 6, 483–494

$^{40}Ar/^{39}Ar$ dating of Miocene tuffs from the Styrian part of the Pannonian Basin: an attempt to refine the basin stratigraphy

ROBERT HANDLER[1,2,*], FRITZ EBNER[3], FRANZ NEUBAUER[1], ANA-VOICA BOJAR[4] and SIEGFRIED HERMANN[5]

[1]Division General Geology and Geodynamics, Department Geography and Geology, University Salzburg, Hellbrunner Str. 34, A-5020 Salzburg, Austria
[2]Present address: Forstinger+Stadlmann ZT-OEG, Achenpromenade 14, A-5081 Anif, Austria; *✉ ro-handler@aon.at
[3]Department of Applied Geosciences and Geophysics, University of Leoben, Peter-Tunner-Str. 5, A-8700 Leoben, Austria
[4]Institute for Earth Sciences, Geology and Paleontology, Karl-Franzens University Graz, Heinrichstr. 26, A-8010 Graz, Austria
[5]GeolithConsult, Frauentalerstr. 51, A-8530 Deutschlandsberg, Austria

(Manuscript received September 19, 2005; accepted in revised form June 22, 2006)

Abstract: In this study we present new $^{40}Ar/^{39}Ar$ age data obtained from volcaniclastic material intercalated within shallow-marine to neritic sediments of the Styrian part of the Miocene Paratethyan Sea, which allow a better control of the sedimentation. At Retznei quarry, a volcaniclastic layer has been deposited in erosional patches above a consolidated rhodolite limestone ("Leitha Limestone") of the siliciclastic/marine Badenian Weissenegg Formation. Ar-release plots of a biotite bulk-grain concentrate (30 grains) and a concentrate of three sanidine crystals (0.5–1 mm) display fairly flat release-patterns with minor fluctuation in the low-energy gas-release steps. From the statistical point of view the biotite concentrate yielded a high-precision plateau age of 14.21 ± 0.07 Ma, the three sanidine crystals yielded a plateau age of 14.39 ± 0.12 Ma. The radiometric ages obtained match the biostratigraphic record (Upper Lagenide Zone). A drill-core recovered from the well Hörmsdorf, exposes several sand-dominated horizons and two layers of crystal tuff, of the Karpatian Eibiswald Formation. Ar-analyses of one single biotite grain (> 1 mm) from the hanging-wall, another biotite single-grain from the lower tuff both display slightly disturbed Ar-release spectra. However Ar-plateau ages of 15.08 ± 0.09 Ma and 15.22 ± 0.17 Ma, respectively, have been obtained. Volcaniclastic rocks from Pöls are intercalated within the Florian Formation, for which previous authors suggested a Early Badenian age (16.4–ca. 15 Ma according to Rögl 1996). A concentrate of two clear sanidine crystals (0.5–1.0 mm), yielded a perfect Ar-plateau recording an age of 15.75 ± 0.17 Ma, which is more precise than previously published K-Ar results.

Key words: Miocene, Paratethys, Pannonian Basin, volcanism, $^{40}Ar/^{39}Ar$ step-heating.

Introduction

For more than 30 years geochronological investigations have been carried out on Miocene volcanic and volcaniclastic rocks of the Styrian Basin, which is part of the western Pannonian Basin System (Fig. 1). The Neogene Pannonian Basin System belongs to the western Paratethys with a distinct stratigraphy different from the Mediterranean area. Since the early days, several attempts have been made in order to establish a precise Paratethyan timescale by means of correlation of biostratigraphical, geochronological and geomagnetical investigations (e.g. Steininger & Bagdasarjan 1977; Vass & Balogh 1989; Rögl 1996). These early radiometric investigations focused on the occurrence of lava and subvolcanic rocks from stratovolcanoes. Tuffs were rarely investigated because of their widespread alteration, which did not allow the preparation and concentration of sufficient unaltered material for analysis. During the last decades, however, analytical procedures made great progress and now geochronological results with a higher precision can be achieved on smaller samples. This advanced approach made possible not only dating of lava and subvolcanic rocks, but of tuffs as well, as significantly less material — sometimes only one grain — is required to obtain perfect results.

The $^{40}Ar/^{39}Ar$ method of dating seems to be the most suitable tool for dating young volcanic and especially volcaniclastic rocks, because of the following reasons: (1) It is not necessary to correlate isotopic analysis of the volcanic phenocrysts with analysis from whole-rock samples, as is necessary, for instance, in Rb-Sr dating. (2) Because of the higher abundance of potassium compared to trace elements such as uranium, errors obtained from Ar-isotopic analyses are much lower. The errors for zircon fission-track (FT) dating generally range between 5–10 % of the age, whereas in ideal cases errors of less than 1 % can be obtained from $^{40}Ar/^{39}Ar$ analysis. (3) Compared to the conventional K-Ar method of dating, $^{40}Ar/^{39}Ar$ analysis allows an insight into the Ar-isotopic distribution of the grain, namely to see whether or not the isotopic composition within the grain(s) is disturbed or not. Thus, alteration of the volcanic minerals, as well as loss or incorporation of extraneous ^{40}Ar-components can be detected by Ar-release spectra in combination with inverse isochron plots, and therefore data obtained by means of the $^{40}Ar/^{39}Ar$ method are much more reliable compared to conventional K-Ar data.

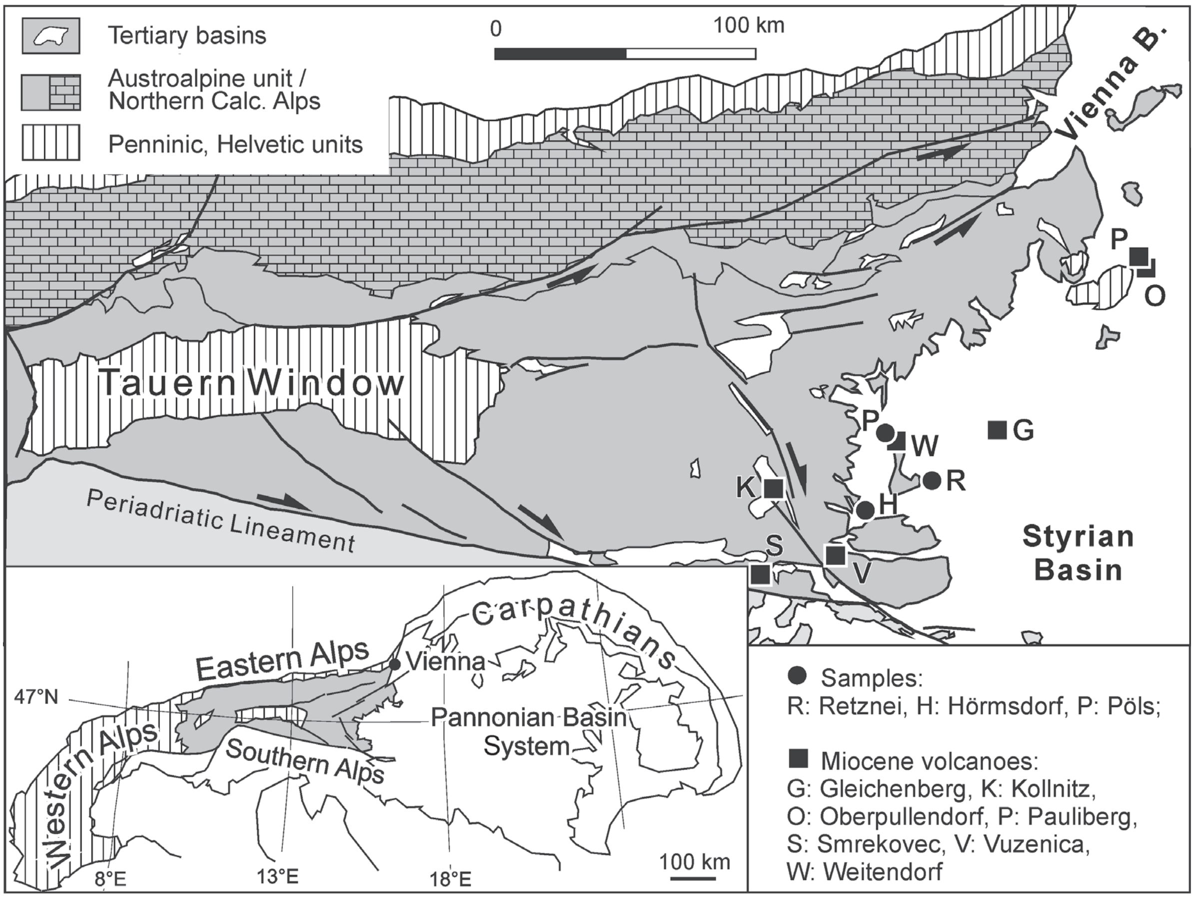

Fig. 1. Simplified map of the Styrian Basin indicating sample locations and position of Miocene volcanoes as possible sources.

First attempts to correlate radiometric ages of tuffs with paleontological and/or stratigraphic investigations have been carried out at the very beginning of this millennium by the Leoben working group (Ebner et al. 2000, 2002). Unfortunately, in the early phases of investigations less attention has been paid to the $^{40}Ar/^{39}Ar$ technique, and fission-track dating of volcanic zircons was their choice for a tephrachronological attempt (e.g. Sachsenhofer et al. 1998; Ebner et al. 2000, 2002). A first attempt to correlate $^{40}Ar/^{39}Ar$ geochronology with $\delta^{18}O$ changes of pectinid and brachiopod shells and global climate change has been carried out in the uppermost rhodolite limestone ("Leitha Limestone") within the Badenian Weissenegg Formation exposed in the Retznei quarry (Bojar et al. 2004).

In this pilot study, we report new data from few Miocene tuffs collected from two surface exposures and a drill hole. The ages show a potential for refining the Paratethyan time-scale calibration by $^{40}Ar/^{39}Ar$ dating of unaltered phenocrysts of tuffs.

Miocene stratigraphy of the Styrian Basin

A short summary of Miocene formations of the Styrian Basin is given in Fig. 2. A detailed description of the evolution of the Styrian Basin has been provided by Ebner & Sachsenhofer (1991). Additionally, more recent studies on the stratigraphy and paleogeography have been published by Rögl (1996, 1998, 2001) and Gross (2000). Sedimentation within the western Styrian Basin started with terrestrial, fluviatile-limnic Ottnangian–Karpatian sedimentary formations, which are followed by shallow-marine, mostly siliciclastic, neritic formations. Within the uppermost Karpatian and lower to middle sectors of the Badenian formations, a few major stratovolcanoes or shield volcanoes, are intercalated. The most important ones are those of Weitendorf and Gleichenberg, and the huge, buried volcanic bodies of Walkersdorf and Mitterlabill, the latter forming the western continuation of the Gleichenberg volcano. Thin, heavily altered, tuffs and bentonite horizons are widespread in shallow-marine sedimentary rocks (Ebner 1981). Stratigraphically upwards along intra-basin swells, the Weissenegg Formation with the "Leitha Limestone" as the hanging-wall member belong to the Lagenide Zone of Badenian age.

Previous geochronology on Miocene volcanic and volcaniclastic rocks in the Styrian Basin and adjoining areas

Geochronological analyses of volcanic and volcaniclastic rocks have a long tradition in the Styrian Basin. A summary of previous radiometric data on volcanic and volcaniclastic rocks is provided in Table 1.

One problem regarding old ages is, that in the early days of geochronology other ^{40}K-decay constants than today were used. Therefore, for a detailed and refined calibration of the stratigraphy these "old" data have to be recalculated with the "new" decay constants suggested by the IUGS Subcommission on Geochronology (Steiger & Jäger 1977). Unfortunately, in some publications analytical details, such as the decay constant used for age-calculation, or the abundances of ^{40}Ar*, or the ^{40}K/^{40}Ar ratio were not reported, and, therefore, these analyses cannot be recalculated to "modern" decay constants.

Thirty years ago Lippolt et al. (1975) was the first to publish K-Ar ages on Miocene volcanics from various sampling sites in Styria and the adjoining Lavant Valley in Carinthia. These first results outlined the importance and the possibility to combine geochronological data with results from paleontological investigations in order to establish a stratigraphic scheme for this area.

In the following (see also Table 1) we briefly summarize the age constraints on Miocene volcanic and volcaniclastic rocks mainly to show possible sources for the tuff layers under consideration and to allow comparison with previous results.

Gleichenberg/SE-Styria

The earliest age reported for the Gleichenberg volcano was presented by Lippolt et al. (1975), but unfortunately only as a "preliminary result" without any analytical details. Therefore, the age of "ca. 14.6 Ma" (Lippolt et al. 1975) cannot be recalculated. Steininger & Bagdasarjan (1977) published four ages obtained from two samples of trachyandesite sampled in the quarry "Klause" north of Gleichenberg. Their results, as above calculated with the "old" decay constants, range between 15.4–17.5 Ma. Recalculation of their analytical results yielded ages of 15.4 and 15.8 Ma for the hanging-wall and 15.4 and 16.8 Ma for the lower part of the quarry.

A further attempt to date the Gleichenberg volcano has been carried out by Kolmer (1980), who calculated a Rb-Sr errorchron age from four whole-rock samples of different volcanic rocks collected at various localities around

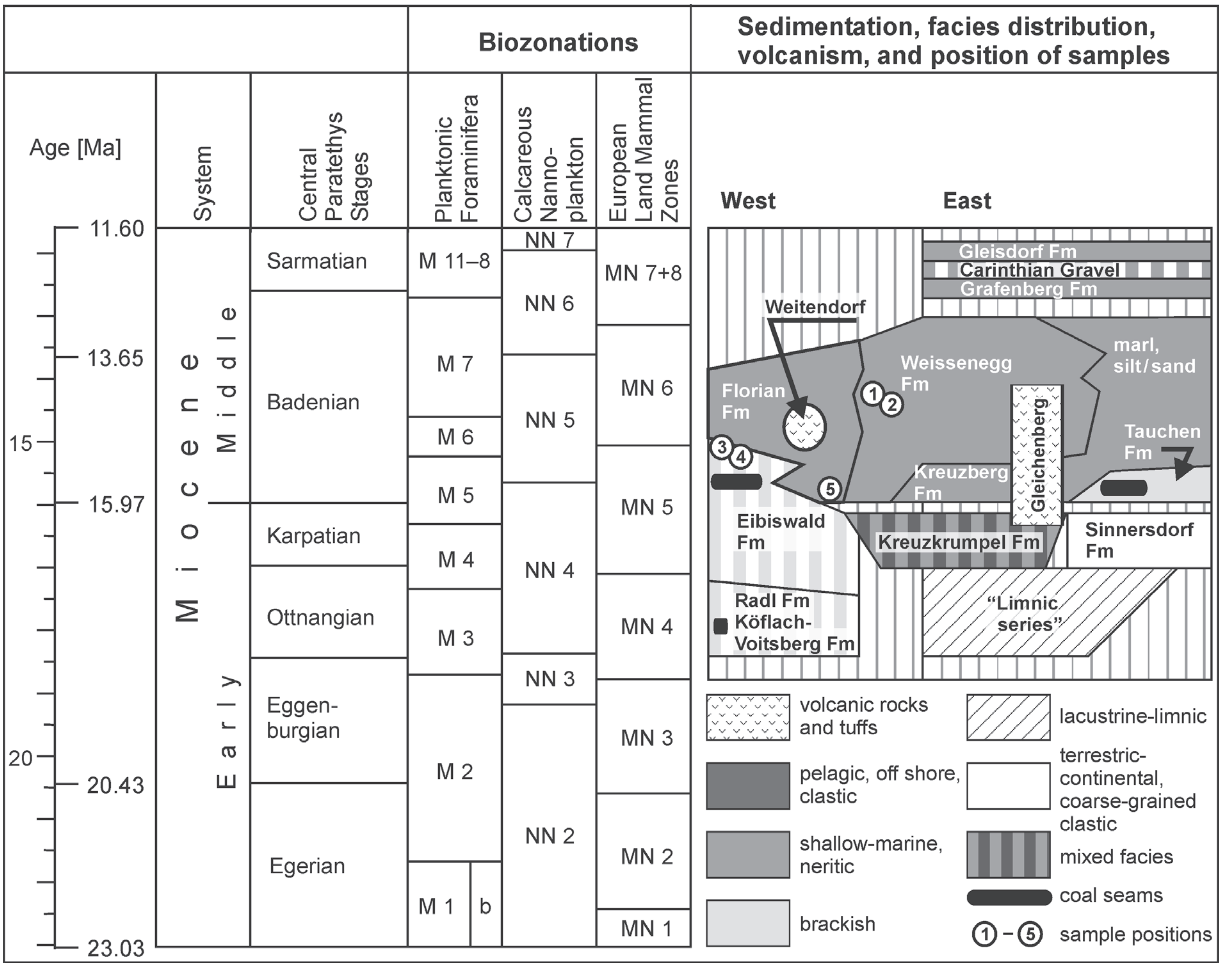

Fig. 2. Sedimentation, facies distribution, volcanism, and position of the samples analysed. Radiometric ages, Central Paratethyan stages, and lithostratigraphic formations according to "The Stratigraphic Table of Austria" (Piller et al. 2004). Biozonations follow Steininger & Wessely (2000), which is based on earlier work by Berggren et al. (1995), Steininger et al. (1996) and Steininger (1999).

Table 1: Compilation of geochronologic investigations (WR = whole rock, FT = fission track) on Miocene volcanic and volcaniclastic rocks in the Styrian Basin and adjoining areas.

Locality	Lithology	Method and Material	Radiometric Age [Ma]	Reference
SE-Styria:				
Gleichenberg	Trachyte	K-Ar WR	14.6[1]	Lippolt et al. (1975)
Quarry Klause/N Bad Gleichenberg	Trachyandesite, lower level	K-Ar WR	(16.1/15.4)[2] 15.4[3] (17.5/17.2)[2] 16.8[3]	Steininger & Bagdasarjan (1977)
Quarry Klause/N Bad Gleichenberg	Trachyandesite, upper level	K-Ar WR	(16.5/15.6)[2] 15.8[3] (16.1/15.5)[2] 15.4[3]	Steininger & Bagdasarjan (1977)
Gleichenberg	4 different volcanic rocks	Rb-Sr WR	22.97 ± 1.93[1]	Kolmer (1980)
Quarry Gossendorf/N Bad Gleichenberg	"Styrian Trass"	K-Ar WR 100–500 µm	13.2 ± 1.0	Balogh et al. (1994)
SW-Styria:				
Quarry Weitendorf	Shoshonite	K-Ar WR 200–500 µm	15.2 ± 0.9 [1]	Lippolt et al. (1975)
Quarry Weitendorf	Shoshonite, lower level	K-Ar WR	(16.8/16.0)[2] 16.1[3] (17.0/16.1)[2] 16.3[3] (18.2/17.7)[2] 17.5[3] (18.0/17.4)[2] 17.3[3]	Steininger & Bagdasarjan (1977)
Quarry Weitendorf	Shoshonite, upper level	K-Ar WR	(16.8/16.0)[2] 16.1[3] (17.4/16.5)[2] 16.6[3] (16.5/15.6)[2] 15.8[3]	Steininger & Bagdasarjan (1977)
Quarry Weitendorf	Latite, lower SW-corner	K-Ar WR	14.0 ± 0.7	Balogh et al (1994)
Quellgraben near Pöls	Hanging-wall tuff of the Florian Fm	K-Ar biotite	16.6 ± 0.6	Balogh et al. (1994)
Quellgraben near Pöls	Foot-wall tuff, 1 m below sample above	K-Ar biotite	15.3 ± 0.9 14.9 ± 0.7	Balogh et al. (1994)
Ratsch	Volcanogenic contaminated sandstone	Zircon FT	15.4 ± 0.5	Ebner et al. (2002)
W-Styria:				
Tregistsattel E Oberdorf	Tuff/Eckwirtschotter	K-Ar biotite	17.5 ± 2.6	Balogh et al. (1994)
Tregistsattel E Oberdorf	Lobmingberg SFm/ Stallhofen Fm	Zircon FT	16.0 ± 0.7	Ebner et al. (2000)
Oberdorf	Tuff/Köflach-Voitsberg Fm	Zircon FT	18.7 ± 0.9	Ebner et al. (2002)
Upper Styria:				
Apfelberg	Tuff/Apfelberg Fm	Zircon FT	15.5 ± 0.8	Ebner et al. (2002)
Flatschach	Tuff/Ingering Fm	Zircon FT	14.9 ± 0.7	Ebner et al. (2002)
Laas	Tuff/Fohnsdorf Fm	Zircon FT	17.1 ± 0.7	Ebner et al. (2002)
Carinthia:				
Quarry Kollnitz near St. Paul i. Lavant Valley	Contaminated basaltic andesite	K-Ar WR 200–500 µm	17.0 ± 4.2[1] 19.6 ± 2.2[1]	Lippolt et al. (1975)
Quarry Kollnitz near St. Paul i. Lavant Valley	Basaltic andesite	K-Ar WR 200–500 µm	14.9 ± 0.9[1]	Lippolt et al. (1975)
Burgenland:				
Quarry Oberpullendorf	Olivine-tholeiitic basalt	K-Ar WR	11.1 ± 1.2	Balogh et al. (1994)
Quarry Pauliberg	Alkali basalt from higher level	K-Ar WR 100–500 µm	10.5 ± 1.0	Balogh et al. (1994)
Quarry Pauliberg	Diabas at lower level	K-Ar WR 100–500 µm	12.3 ± 1.1 11.7 ± 0.4 11.0 ± 0.5	Balogh et al. (1994)
Slovenia:				
Vuzenica	Dacite dyke	Apatite FT	14.6 ± 1.8	Sachsenhofer et al. (1998)
Smrekovec	Volcanite	K-Ar WR	22.0 ± 2.1 22.3 ± 1.0 27.4 ± 2.7 27.6 ± 2.4	Hanfland et al. (2004)

[1]) Analytical details, as the decay constant used for age calculation, are not given by the authors. The significance of the reported age is therefore questionable.
[2]) Ages as calculated by Steininger & Bagdasarjan (1977) who used a decay constant of $\lambda_{K\text{-}40}$ = 0.557E-10/0.585E-10 respectively.
[3]) For the present study recalculated ages from analytical data given by the authors using today accepted decay constants reported by the IUGS Subcommission on Geochronology (Steiger & Jäger 1977).

Gleichenberg. The rather obscure result was an age of 22.97 ± 1.93 Ma.

On the northern flank of the Gleichenberger Kogel stratovolcano near Gossendorf the trachyte/trachyandesite is completely converted to opal, alunite, and clays due to post-volcanic hydrothermal activity. For this alteration product, the so-called "Styrian Trass" a K-Ar whole-rock age of 13.2 ± 1.0 Ma was determined by Balogh et al. (1994).

Weitendorf/SW-Styria

Circa 3.5 km ESE of Weitendorf, near Wildon, a shoshonite is excavated in an open-pit quarry. There, volcanic rocks are intercalated within fine-clastic sediments. Occurrences of fossil-bearing marly clay can be found as intercalations within, as well as both in the hanging- and footwall of the volcanic body. This interesting and rather rare situation suggests that this occurrence is an ideal site for paleontological-geochronological correlations. However, the age and nature of this volcanic body have been a matter of debate, due to contrasting observations and interpretations (see Ebner & Gräf 1977, and Krainer 1987 for summaries of older literature). On the basis of fritted margins and thermally induced bleaching effects, slickensides in the footwall and local steep inclinations of adjacent sediments, as well as the presence of local pillow-structures, today's most accepted theory is that the volcanic body intruded as a sill into the wet marine sediments near the hydro-/lithosphere boundary (Krainer 1987).

From the footwall sediments, Ebner & Gräf (1977) and Fenninger & Wassermann (1982) described a rich marine macro-fauna, which suggests a Badenian age (Upper Lagenide Zone). Krainer (1987) found similar heavy-mineral assemblages in the foot- and hanging-wall mudstones, and a rich micro-fauna in the hanging-wall sediments, and interpreted his data to support a model of either emplacement of the shoshonite as a sill within the sediments, or at least rapid coverage of the shoshonite with marine sediments. In any case, a Badenian age (Upper Lagenide Zone) is well constrained by paleontological data.

The first geochronological results regarding Styrian volcanic rocks were obtained from the Weitendorf quarry. Lippolt et al. (1975) reported an age of 15.2 ± 0.9 Ma for K-Ar analyses performed on the 200–500 μm size-fraction of a whole-rock sample. Unfortunately, the authors did not give any analytical details, and therefore it is difficult to judge the reliability of this datum, or to recalculate the age. Steininger & Bagdasarjan (1977) published seven ages obtained from two samples. Their results range between 16.0–18.2 Ma calculated with the "old" decay constants. Recalculation of their analytical results yielded ages still within a large range of 16.1–17.51 Ma for the hanging-wall and 15.8–16.6 Ma for the lower part of the quarry.

The most recent age data have been obtained by Balogh et al. (1994), who reported a series of K-Ar whole-rock data from various areas within the Styrian Basin. They obtained ages of 14.0 ± 0.7 Ma for the shoshonite/latite exposed in the Weitendorf quarry.

Summing up, the ages reported span over a period of 4 Myr (see Table 1) and range between 14.0 Ma (Balogh et al. 1994) and 18.0 Ma (Steininger & Bagdasarjan 1977).

Kollnitz near St. Paul/Carinthia

In the Lavant Valley of southeastern Carinthia a basalt was quarried near the village Kollnitz. The first ages were obtained by Lippolt et al. (1975), who reported ages of 14.9 ± 0.9, 17.0 ± 4.2 and 19.6 ± 2.2 Ma, the latter two from a contaminated basalt. Therefore, the youngest age of 14.9 ± 0.9 Ma is interpreted as geologically significant. However, due to the lack of detailed analytical data a recalculation of the age with recently accepted decay constants is not possible.

Pauliberg and Oberpullendorf/Burgenland

Balogh et al. (1994) reported K-Ar whole-rock ages of 10.5 ± 1.0 Ma for an alkali-basalt (Dobosi et al. 1991) from the hanging-wall part of the quarry at Pauliberg, and ages of 11.0 ± 0.5, 11.7 ± 0.4, and 12.3 ± 1.1 Ma for the diabase at the base of the quarry. Based on interpretations of "classical" Ar-isochron plots (i.e. $^{40}Ar/^{36}Ar$ vs. $K/^{36}Ar$), these authors suggest an age of ca. 11.5 Ma as the "most probable" age for the volcanics from Pauliberg.

A K-Ar whole-rock age of 11.1 ± 1.2 Ma is reported for an olivine-tholeiitic basalt from the lower levels in the old quarry of Oberpullendorf (Balogh et al. 1994). Despite the fact that extraordinarily high amounts of gas have been obtained from this sample, which might indicate excess-Ar components, the authors interpret this age as geologically meaningful, because it is within the same range as ages obtained for the nearby Pauliberg volcanics.

Eastern Pohorje Mts/Slovenia

Sachsenhofer et al. (1998) reported an apatite fission-track age of 14.6 ± 1.8 Ma for a dacite dyke from the area of Vuzenica, Slovenia. Because the tracks show very minor shortening, these authors conclude that the depth of emplacement was shallow or exhumation took place soon after volcanic activity. Vitrinite reflectance and FT data on detrital apatite from adjoining Tertiary sedimentary rocks, however, indicate a thermal overprint with a mean age of 14.4 ± 2.3 Ma, which is within error to the age reported from the dacite. Therefore, the age reported for the Vuzenica dyke can only be regarded as a minimum age for the volcanic activity.

Smrekovec volcano/Slovenia

An older period of magmatic activity is reported for the Smrekovec volcano, Slovenia. Hanfland et al. (2004) reported Oligocene/Early Miocene K-Ar ages obtained from whole-rock analyses ranging between ca. 22 and 29 Ma. Because of the intense hydrothermal alteration, the authors suspect Ar-loss and interpret their ages as minimum ages for volcanic activity.

Previous geochronology on Styrian tuffs

From the locality Quellgraben near Pöls, two layers of bentonite are intercalated within, and separated by ca. 1 m thick marine sedimentary rocks of the Florian Formation. These marls belong to the Lagenide Zone of the Lower Badenian. K-Ar analysis on volcanic biotite has been carried out by Balogh et al. (1994). For the lower sample these authors report ages of 14.9 ± 0.7 Ma and 15.3 ± 0.6 Ma (with the reported mean age of 15.1 ± 0.5 Ma). Biotite from the second sample, which is 1 m in the hanging-wall, yielded an age of 16.6 ± 0.6 Ma. It is interesting to note, that the stratigraphic younger layer contains older biotite. A significantly older K-Ar age of 17.5 ± 2.6 has been reported for a concentrate of biotite from tuff-layer exposed in the area around Köflach/Voitsberg (Balogh et al. 1994). From the same area Ebner et al. (2000, 2002) reported zircon fission-track ages of 16.0 ± 0.7 Ma and 18.7 ± 0.9 Ma which fit well with similar ages obtained by the same technique of 14.9 ± 0.7 Ma, 15.5 ± 0.8 Ma, and 17.1 ± 0.7 Ma for tuffs deposited within the "Noric Depression" of Upper Styria (Ebner et al. 2000, 2002), and another zircon fission-track age of 15.4 ± 0.5 Ma from a volcanogenic contaminated sandstone exposed near Ratsch in the southwestern part of Styria (Ebner et al. 2002).

Sample location and description

Retznei (samples 1 and 2)

The "Retznei Zementwerk" quarry has been described in detail by Friebe (1990, 1991), Fritz & Hiden (2001) and Bojar et al. (2004). A first description of volcanic rocks within the sedimentary succession exposed in the quarry of Retznei can be found in Hauser (1951), who describes an "andesite" in the hanging-wall part of this quarry. Friebe (1990) described two tuffite layers below the above mentioned "andesite". The lower tuffite is intercalated in between a rhodolite limestone of the Badenian Weissenegg Formation (= "Leitha Limestone"), the younger was deposited above the limestone, at the base of the sand-dominated top exposed in the quarry. Both tuffite layers show a variable degree of detrital influx. Still in the hanging-wall of the latter, a biotite-rich volcanic layer, which was first described as an andesite by Hauser (1951), is exposed. Today it is accepted that Hauser's andesite is a pyroclastic rock, which has been deposited in erosional patches above the consolidated limestone. Gravitational slumping structures can be recognized and are explained to be due to deposition of the tuff on the slope of the reef flanks of the "Leitha Limestone". In contrast to the two tuffite layers in the footwall of this layer, no contribution of other detrital minerals has been recognized within that layer. Therefore we believe that this sample represents a real tuff rather than a tuffite. The tuff itself is almost unconsolidated, inspite of local weathering products, as indicated by the occurrence of montmorillonite. Although weathered, it was possible to separate one fresh biotite (sample 1 = AVB2 of Bojar et al. 2004) and one fresh, coarse-grained sanidine (sample 2) concentrate.

Well Hörmsdorf (samples 3 and 4)

Near the village Eibiswald, a drilling project of the Graz-Köflach-Railway (GKB) has been carried out (well Hörmsdorf 3). The complete core with a diameter of ca. 7 cm has been sampled. The drilling reached the pre-Tertiary basement at a final depth of 265 m. The basement is overlain by the Eibiswald Formation for which a Karpatian age is assumed. A lithostratigraphic description is provided by Gruber et al. (2003) and summarized in Fig. 3. The lower 70 cm of the core comprise massive, coarse conglomerates of the Lower Eibiswald Formation. These strata are interpreted as mass flows and turbidites. In the hanging-wall, the massive conglomerates become layered with intercalations of more fine-clastic sedimentary rocks. The basal succession contains a ca. 30 cm thick layer of coal. A few meters above the coal-horizon several sand dominated horizons and two layers of crystal tuff are intercalated. From each of these layers one biotite concentrate has been prepared. Sample 3 has been sampled at the basis of a well consolidated, ca. 10 cm thick layer of light, not consolidated, laminated sands in the hanging-wall of dark brown clay-silt material. The biotite grains from this tuff layer are not altered and show no inclusions. Sample 4 has been prepared from a ca. 20 cm thick tuff layer a few meters above sample 3. The largest biotite crystals in this layer reach diameters up to 2 mm.

Pöls (sample 5)

Volcanic tuffs south of the village Pöls have been described by Kopetzky (1957). Two different layers are intercalated within the shallow marine fine clastic Lower Badenian Florian Formation which contains foraminifers and rich mollusc faunas. From one of these tuff layers a concentrate of clear, coarse-grained sanidine has been prepared.

Analytical techniques

Mineral concentrates are packed in aluminium-foil and loaded in quartz vials. For calculation of the J-values, flux-monitors are placed between each 4–5 unknown samples, which yield a distance of ca. 5 mm between adjacent flux-monitors. The sealed quartz vials are irradiated in the MTA KFKI reactor (Debrecen, Hungary) for 16 hours. Correction factors for interfering isotopes have been calculated from 10 analyses of two Ca-glass samples and 22 analyses of two pure K-glass samples, and are: $^{36}Ar/^{37}Ar_{(Ca)} = 2.6025E\text{-}4$, $^{39}Ar/^{37}Ar_{(Ca)} = 6.5014E\text{-}4$, and $^{40}Ar/^{39}Ar_{(K)} = 1.5466E\text{-}2$. Variations in the flux of neutrons were monitored with DRA1 sanidine standard for which a $^{40}Ar/^{39}Ar$ plateau age of 25.03 ± 0.05 Ma has been reported (Wijbrans et al. 1995). After irradiation the minerals are unpacked from the quartz vials and the aluminium-foil packets, and handpicked into 1 mm diameter holes within one-way Al-sample holders.

$^{40}Ar/^{39}Ar$ analyses are carried out at the *ARGONAUT*-Laboratory of the University of Salzburg using a UHV Ar-extraction line equipped with a combined MERCHANTEK^{TM} UV/IR laser ablation facility, and a VG-ISOTECH^{TM} NG3600 Mass Spectrometer.

Stepwise heating analyses of samples are performed using a defocused (~1.5 mm diameter) 25 W CO_2-IR laser operating in Tem_{00} mode at wavelengths between 10.57 and 10.63 µm. The laser is controlled from a PC, and the position of the laser on the sample is monitored through a double-vacuum window on the sample chamber via a video camera in the optical axis of the laser beam on the computer screen. Gas clean-up is performed using one hot and one cold Zr-Al SAES getter. Gas admittance and pumping of the mass spectrometer and the Ar-extraction line are computer controlled using pneumatic valves. The NG3600 is a 18 cm radius 60º extended geometry instrument, equipped with a bright NIER-type source operated at 4.5 kV. Measurement is performed on an axial electron multiplier in static mode, peak-jumping and stability of the magnet is controlled by a Hall-probe. For each increment the intensities of ^{36}Ar, ^{37}Ar, ^{38}Ar, ^{39}Ar, and ^{40}Ar are measured, the baseline readings on mass 35.5 are automatically subtracted. Intensities of the peaks are back extrapolated over 16 measured intensities to the time of gas admittance either by a straight line or a curved fit. Intensities are corrected for system blanks, background, post-irradiation decay of ^{37}Ar, and interfering isotopes. Isotopic ratios, ages and errors for individual steps are calculated following suggestions by McDougall & Harrison (1999) using decay factors reported by Steiger & Jäger (1977). Definition and calculation of plateau ages has been carried out using ISOPLOT/EX (Ludwig 2001). For inverse isotope correlation diagrams regression algorithms of York (1969) are used.

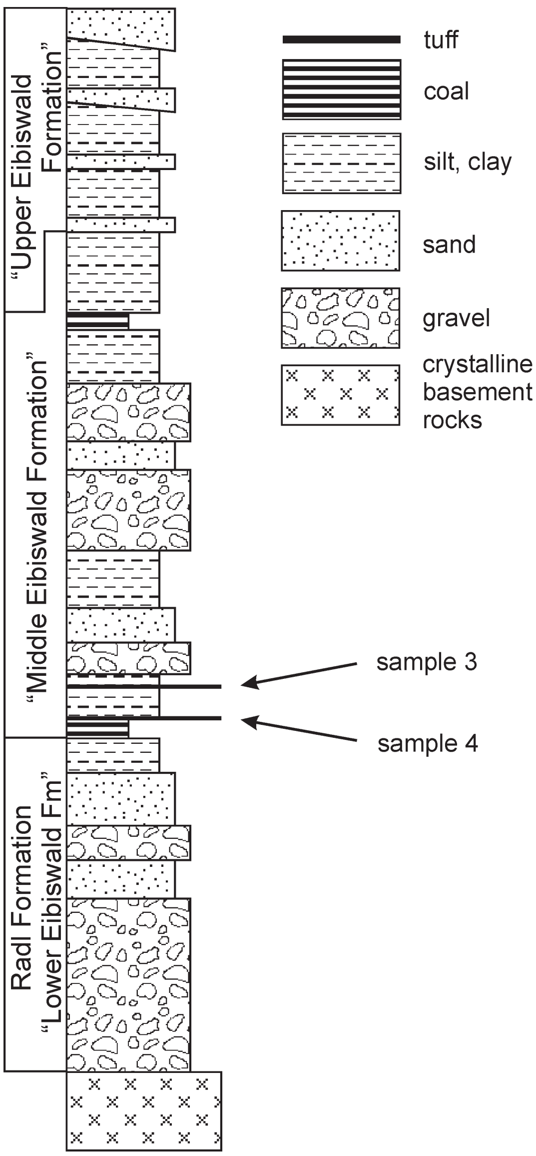

Fig. 3. Sequence of strata within the Eibiswald Formation including the Hörmsdorf well with the two tuff layers dated (modified after Gruber et al. 2003).

$^{40}Ar/^{39}Ar$ ages of Miocene tuffs

Analytical results from incremental heating experiments of the biotite and sanidine samples are provided in Table 2 and graphically presented as Ar-release spectra in Fig. 4. In general all dated samples display well defined plateau-ages. To allow control of the possible contribution of excess-Ar components to the Ar-isotopic system of the material analysed, inverse isotope correlation diagrams have been included in Fig. 4. Although seldom justified, because the probability of fit of the regression is seldom more than 15 %, generally *Model 1* solutions have been selected, because *Model 2* regressions assign equal weights to the individual data points and ignore the individual data point errors. Despite the discussion which type of regression model should be used, it is worth noting, that the inverse isochron plots do not display any sign of excess-Ar incorporation in any of the analysed samples. In the following, the results are discussed according to their sample location and stratigraphic age.

Reztnei

One biotite (125–250 µm) bulk-grain concentrate of 30 grains (sample 1), and a concentrate of three large (0.5–1.0 mm) sanidine crystals (sample 2) have been analysed. Ar-release plots of both concentrates display fairly flat release-patterns with minor fluctuation in the low-energy gas-release steps. However, both samples display well defined plateau-ages, which are similar within error. From the statistical point of view, biotite sample 1 yielded a high-precision age of 14.21 ± 0.07 Ma recorded in steps 11–18 (fusion), which together comprise 77.3 % of the ^{39}Ar released. Fluctuations in the first, low energy gas-release steps are not matched by $^{37}Ar/^{39}Ar$ variations.

Table 2: Ar-analytical data for incremental heating-experiments on biotite and sanidine samples from Miocene tuffs of the western part of the Pannonian Basin (Styria, Austria). *Continued on the next page.*

Sample 1: Biotite 125–250 μm, 30 grains (J-value: 0.02219 ± 0.00022)

Step	$^{36}Ar/^{39}Ar^{a}$	±	$^{37}Ar/^{39}Ar^{b}$	±	$^{40}Ar/^{39}Ar^{a}$	±	$^{39}Ar/^{40}Ar^{c}$	±	$^{36}Ar/^{40}Ar^{a}$	±	$\%^{40}Ar^{d}$	$\%^{39}Ar$	age	± [Ma]
1	0.05582	0.00041	0.31034	0.00017	16.77512	0.12279	0.05966	0.00005	0.00333	0.00002	1.7	0.5	11.6	4.9
2	0.05321	0.00024	0.17454	0.00008	16.01414	0.07155	0.06250	0.00004	0.00332	0.00001	1.8	0.7	11.5	2.8
3	0.02984	0.00021	0.00779	0.00011	9.15006	0.06254	0.10947	0.00005	0.00326	0.00002	3.6	0.9	12.7	2.5
4	0.00067	0.00030	0.85993	0.00034	0.48308	0.08803	2.13726	0.00864	0.00140	0.00062	58.8	0.3	13.4	3.5
5	0.00034	0.00014	0.44017	0.00016	0.51220	0.04024	2.01254	0.00380	0.00067	0.00027	80.3	0.6	17.1	1.6
6	0.00036	0.00008	0.20920	0.00008	0.50397	0.02343	2.04677	0.00221	0.00072	0.00016	78.6	1.2	15.8	0.9
7	0.00020	0.00003	0.14863	0.00004	0.46466	0.00925	2.22598	0.00139	0.00042	0.00007	87.5	2.6	16.0	0.4
8	0.00066	0.00004	0.32920	0.00004	0.52093	0.01263	1.97795	0.00137	0.00126	0.00008	62.8	1.9	13.4	0.5
9	0.00028	0.00002	0.17169	0.00002	0.43007	0.00454	2.41164	0.00088	0.00066	0.00004	80.5	5.0	13.7	0.2
10	0.00022	0.00001	0.14481	0.00001	0.40970	0.00324	2.53634	0.00063	0.00054	0.00003	84.0	8.9	13.6	0.2
11	0.00017	0.00001	0.14343	0.00001	0.41137	0.00260	2.52561	0.00059	0.00041	0.00002	87.9	10.0	14.2	0.2
12	0.00014	0.00001	0.11637	0.00001	0.39894	0.00178	2.60751	0.00052	0.00035	0.00002	89.6	11.6	14.0	0.2
13	0.00011	0.00001	0.13726	0.00001	0.39642	0.00375	2.62472	0.00083	0.00027	0.00003	92.0	6.7	14.3	0.2
14	0.00011	0.00001	0.05569	0.00001	0.40050	0.00300	2.59706	0.00056	0.00026	0.00003	92.2	11.1	14.3	0.2
15	0.00011	0.00001	0.06407	0.00001	0.40171	0.00247	2.58895	0.00044	0.00027	0.00002	92.1	13.6	14.3	0.2
16	0.00011	0.00001	0.06327	0.00001	0.39431	0.00320	2.63951	0.00070	0.00029	0.00003	91.6	10.4	14.0	0.2
17	0.00008	0.00001	0.00354	0.00001	0.39881	0.00437	2.60862	0.00077	0.00019	0.00004	94.3	7.1	14.4	0.2
18	0.00007	0.00001	0.02495	0.00001	0.39006	0.00396	2.66953	0.00085	0.00017	0.00003	94.8	6.8	14.2	0.2
11–18 =	plateau											77.3	14.21	0.07
	total-gas											100.0	14.1	0.1

Sample 2: Sanidine 0.5–1.0 mm, 3 grains (J-value: 0.01660 ± 0.00017)

Step	$^{36}Ar/^{39}Ar^{a}$	±	$^{37}Ar/^{39}Ar^{b}$	±	$^{40}Ar/^{39}Ar^{a}$	±	$^{39}Ar/^{40}Ar^{c}$	±	$^{36}Ar/^{40}Ar^{a}$	±	$\%^{40}Ar^{d}$	$\%^{39}Ar$	age	± [Ma]
1	0.00445	0.00052	2.17451	0.00110	1.37429	0.15317	0.73488	0.00205	0.00324	0.00038	4.4	0.6	6.4	4.6
2	0.00240	0.00034	2.29166	0.00048	0.93945	0.10193	1.08064	0.00267	0.00255	0.00037	24.6	1.0	11.7	3.0
3	0.00209	0.00017	2.37405	0.00037	0.81028	0.04916	1.25618	0.00184	0.00258	0.00021	23.7	2.3	10.7	1.5
4	0.00138	0.00013	2.45966	0.00033	0.60865	0.03766	1.68304	0.00240	0.00227	0.00021	33.0	2.5	11.2	1.1
5	0.00109	0.00006	2.36286	0.00018	0.57005	0.01688	1.80029	0.00105	0.00190	0.00010	43.7	6.7	12.4	0.5
6	0.00087	0.00006	2.53368	0.00019	0.56257	0.01839	1.82472	0.00131	0.00154	0.00011	54.4	6.0	14.5	0.6
7	0.00090	0.00005	2.47125	0.00012	0.58957	0.01421	1.73897	0.00079	0.00152	0.00008	55.1	8.7	14.9	0.4
8	0.00096	0.00001	2.59029	0.00004	0.58209	0.00352	1.76180	0.00026	0.00165	0.00002	51.1	42.7	14.4	0.2
9	0.00093	0.00004	2.57600	0.00011	0.55637	0.01070	1.84556	0.00081	0.00166	0.00007	50.9	9.7	13.9	0.3
10	0.00096	0.00006	2.62507	0.00021	0.55617	0.01641	1.84621	0.00138	0.00172	0.00010	49.0	5.7	13.7	0.5
11	0.00079	0.00003	2.56209	0.00010	0.54520	0.00783	1.88450	0.00078	0.00146	0.00005	56.9	14.1	14.7	0.3
6–11 =	plateau											86.9	14.39	0.12
	total-gas											100.0	14.0	0.1

Sample 3: Biotite >1 mm, 1 grain (J-value: 0.02220 ± 0.00022)

Step	$^{36}Ar/^{39}Ar^{a}$	±	$^{37}Ar/^{39}Ar^{b}$	±	$^{40}Ar/^{39}Ar^{a}$	±	$^{39}Ar/^{40}Ar^{c}$	±	$^{36}Ar/^{40}Ar^{a}$	±	$\%^{40}Ar^{d}$	$\%^{39}Ar$	age	± [Ma]
1	0.001800	0.000195	0.033973	0.000159	1.268305	0.057566	0.798169	0.000954	0.001419	0.000154	58.1	0.8	28.8	2.3
2	0.001242	0.000114	0.042730	0.000084	0.910669	0.033684	1.117033	0.000957	0.001364	0.000125	59.7	1.6	21.2	1.3
3	0.000973	0.000047	0.016326	0.000034	0.683940	0.013897	1.495928	0.000679	0.001423	0.000069	58.0	4.3	15.2	0.6
4	0.001150	0.000042	0.007875	0.000035	0.716297	0.012335	1.426871	0.000593	0.001605	0.000058	52.6	4.4	14.4	0.5
5	0.010213	0.000114	0.018567	0.000073	3.510207	0.033676	0.286141	0.000123	0.002910	0.000032	14.0	2.1	19.0	1.3
6	0.002471	0.000027	0.020855	0.000016	1.128781	0.008113	0.898206	0.000191	0.002189	0.000024	35.3	8.7	15.3	0.4
7	0.000222	0.000029	0.055865	0.000044	0.438346	0.008662	2.364648	0.001519	0.000505	0.000067	85.1	3.5	14.4	0.4
8	0.000170	0.000019	0.013752	0.000028	0.435581	0.005491	2.380276	0.001166	0.000389	0.000043	88.5	5.4	14.8	0.3
9	0.000072	0.000019	0.021904	0.000022	0.417184	0.005581	2.489270	0.001036	0.000174	0.000045	94.9	8.6	15.2	0.3
10	0.000090	0.000013	0.033228	0.000016	0.422611	0.003777	2.456071	0.000862	0.000213	0.000030	93.7	11.6	15.3	0.2
11	0.000088	0.000009	0.021279	0.000009	0.416722	0.002660	2.492140	0.000502	0.000211	0.000022	93.8	18.5	15.0	0.2
12	0.000084	0.000011	0.033959	0.000011	0.411296	0.003107	2.526278	0.000507	0.000205	0.000026	93.9	17.0	14.9	0.2
13	0.000079	0.000040	0.003369	0.000043	0.426769	0.011888	2.431294	0.001736	0.000185	0.000094	94.5	3.9	15.5	0.5
14	0.000011	0.000030	0.013887	0.000038	0.412896	0.008994	2.516144	0.001432	0.000026	0.000074	99.2	4.9	15.8	0.4
15	0.000149	0.000032	0.783773	0.000043	0.636904	0.009360	1.608331	0.000688	0.000235	0.000050	93.1	4.7	25.4	0.4
6–14 =	plateau											82.1	15.08	0.09
	total-gas											100.0	15.8	0.2

Table 2: *Continued.*

Sample 4: Biotite >1 mm, 1 grain (J-value: 0.02221 ± 0.00022)														
Step	$^{36}Ar/^{39}Ar^a$	±	$^{37}Ar/^{39}Ar^b$	±	$^{40}Ar/^{39}Ar^a$	±	$^{39}Ar/^{40}Ar^c$	±	$^{36}Ar/^{40}Ar^a$	±	$\%^{40}Ar^d$	$\%^{39}Ar$	age	± [Ma]
1	0.00332	0.00010	0.39571	0.00009	1.19143	0.03025	0.85015	0.00075	0.00279	0.00009	17.6	3.6	9.0	1.2
2	0.00207	0.00007	0.26205	0.00008	0.79188	0.01993	1.28775	0.00126	0.00261	0.00009	22.8	4.6	7.4	0.8
3	0.00067	0.00002	0.05947	0.00001	0.53323	0.00621	1.93132	0.00055	0.00125	0.00004	63.0	24.4	13.0	0.3
4	0.00066	0.00034	0.58607	0.00030	0.50380	0.10143	2.04698	0.00751	0.00131	0.00068	61.3	1.3	13.5	4.0
5	0.00002	0.00024	0.21893	0.00025	0.43005	0.07163	2.41169	0.00834	0.00005	0.00056	98.4	1.8	16.9	2.8
6	0.00019	0.00011	0.02202	0.00013	0.44166	0.03232	2.34630	0.00413	0.00042	0.00025	87.5	3.6	14.9	1.3
7	0.00020	0.00003	0.07987	0.00004	0.44166	0.00902	2.34623	0.00153	0.00046	0.00007	86.4	13.5	14.9	0.4
8	0.00011	0.00002	0.10536	0.00002	0.42898	0.00530	2.41811	0.00098	0.00026	0.00004	92.2	20.3	15.5	0.3
9	0.00017	0.00003	0.03059	0.00004	0.43377	0.00998	2.39058	0.00174	0.00038	0.00008	88.7	12.2	14.8	0.4
10	0.00001	0.00003	0.01085	0.00004	0.40371	0.00973	2.57568	0.00188	0.00003	0.00008	99.0	11.4	15.4	0.4
11	0.00025	0.00014	0.03638	0.00015	0.45675	0.04175	2.26604	0.00462	0.00055	0.00031	83.7	3.1	14.8	1.7
12	0.00155	0.00105	0.37628	0.00113	0.51266	0.31004	2.01076	0.02120	0.00303	0.00205	10.4	0.4	2.7	12.4
4–12 =	plateau											67.5	15.22	0.17
	total-gas											100.0	14.2	0.1
Sample 5: Sanidine 0.5–1.0 mm, 2 grains (J-value: 0.01656 ± 0.000017)														
Step	$^{36}Ar/^{39}Ar^a$	±	$^{37}Ar/^{39}Ar^b$	±	$^{40}Ar/^{39}Ar^a$	±	$^{39}Ar/^{40}Ar^c$	±	$^{36}Ar/^{40}Ar^a$	±	$\%^{40}Ar^d$	$\%^{39}Ar$	age	± [Ma]
1	0.00188	0.00031	2.28297	0.00072	1.06371	0.09224	0.95254	0.00193	0.00177	0.00029	47.8	2.1	19.9	2.7
2	0.00216	0.00029	2.31597	0.00066	0.74422	0.08461	1.37009	0.00305	0.00290	0.00038	14.3	2.3	8.0	2.5
3	0.00149	0.00019	2.40467	0.00055	0.64821	0.05528	1.57788	0.00315	0.00230	0.00029	32.1	3.6	11.3	1.6
4	0.00063	0.00012	2.56411	0.00031	0.55375	0.03688	1.85456	0.00253	0.00114	0.00023	66.4	5.8	16.4	1.1
5	0.00057	0.00002	2.29284	0.00006	0.52446	0.00627	1.96164	0.00053	0.00109	0.00004	67.8	37.6	15.4	0.2
6	0.00035	0.00014	2.49318	0.00034	0.49301	0.04251	2.09054	0.00370	0.00072	0.00029	78.9	4.2	16.8	1.3
7	0.00036	0.00004	2.36708	0.00012	0.48500	0.01198	2.12641	0.00122	0.00074	0.00008	78.0	14.9	16.2	0.4
8	0.00027	0.00008	2.26778	0.00023	0.46999	0.02362	2.19676	0.00195	0.00058	0.00017	82.9	8.3	16.3	0.7
9	0.00049	0.00005	2.36308	0.00016	0.49948	0.01501	2.06276	0.00149	0.00099	0.00010	70.9	12.4	15.5	0.5
10	0.00032	0.00008	2.21261	0.00020	0.49990	0.02407	2.06122	0.00183	0.00063	0.00016	81.4	8.8	16.7	0.7
4–10 =	plateau											91.9	15.75	0.17
	total-gas											100.0	15.5	0.2

All errors quoted are at 1-sigma level.
a — measured; b — corrected for post-irradiation decay of ^{37}Ar; c — corrected for irradiation induced interfering Ar-Isotopes; d — non-atmospheric ^{40}Ar

Sanidine sample 2, yielded 14.39 ± 0.12 Ma for steps 6–11 (fusion), together comprising 86.9 % ^{39}Ar released. The staircase type pattern of the first five increments displayed in the Ar-release pattern is matched by a slight decrease of the $^{37}Ar/^{39}Ar$ ratio. These first increments are interpreted, therefore, as the result of degassing from a younger, less retentive, mineralogical phase, probably the result of minor weathering, which has been reported from other layers in this quarry.

Well Hörmsdorf

From the two tuff-layers recovered from the Hörmsdorf drill-core, one biotite single-grain (> 1 mm) each has been analysed by step-wise heating technique. The biotite from the hanging-wall (sample 3) displays a slightly disturbed Ar-release spectrum as well, with higher ages reported in the first two and the last increment. However, an Ar-plateau-age of 15.08 ± 0.09 Ma is defined for steps 6–14 (together comprising 82.1 % ^{39}Ar released). The biotite sample 4 from the lower tuff layer again yielded a slightly disturbed Ar-release pattern. The first two increments might indicate minor alteration of the sample, and are matched by slightly higher $^{37}Ar/^{39}Ar$ ratios. Therefore, we interpret these ages at around 9 Ma to reflect degassing of a younger, less retentive, more Ca-rich mineralogical phase. However, for steps 4–12 (fusion), which together comprise 67.5 % of the ^{39}Ar released, a plateau age of 15.22 ± 0.17 Ma can be calculated.

Pöls

One concentrate (sample 5) containing two sanidine crystals (0.5–1.0 mm) has been analysed. Results yielded a perfect plateau-type of the Ar-release pattern. For steps 4–10 (fusion), together comprising 91.9 % ^{39}Ar released, a plateau age of 15.75 ± 0.17 Ma has been calculated. This age fits perfectly with the previously published ages of 16.6 ± 0.6 Ma and 15.1 ± 0.5 Ma obtained from K-Ar dating of biotite by Balogh et al. (1994).

Discussion

Generally no incorporation of excess Ar components is indicated by Ar-release spectra nor isotope correlation plots, and no significant loss of radiogenic Ar components is indicated in the low-energy gas-release steps. Therefore

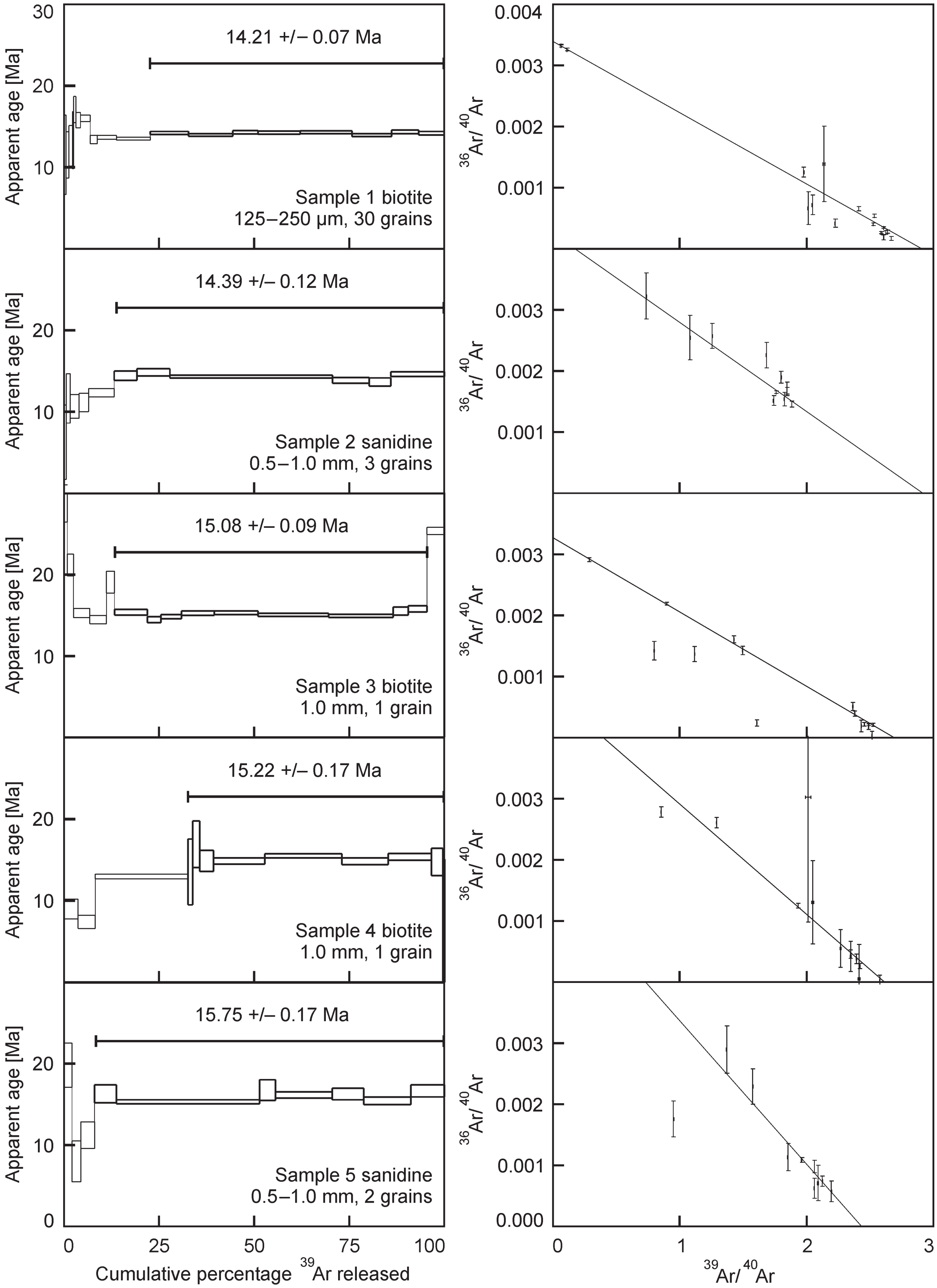

Fig. 4. Ar-release spectra, and isotope correlation plots of biotite and sanidine concentrates dated. Steps used for calculation of ages in the Ar-release plots are indicated by bars, errors are at 1-sigma inter-laboratory level. In isotope correlation plots error-crosses on data points represent 1-sigma errors.

the ages presented in this study are interpreted as reflecting rapid cooling subsequent to volcanic eruptions.

Results from the Badenian tuffs in the hanging-wall of the "Leitha Limestone" of the Weissenegg Formation exposed in the quarry Retznei match the biostratigraphic record (Upper Lagenide Zone) as described by Friebe (1990) and correlate with published biostratigraphic data such as that proposed by Rögl (1996).

The data from the Hörmsdorf well are of particular importance for the age classification of coal occurrences in the Styrian Basin. Three huge coal deposits exist along the western margins of the Miocene Pannonian Basin. The oldest is the Köflach-Voitsberg deposit, for which mostly an Ottnangian, for uppermost sequences a Karpatian, age is discussed (Steininger et al. 1998). The Eibiswald and Wies coal-deposits are of Badenian age, with the Eibiswald is in an intermediate position and the Wies deposit representing the uppermost and youngest deposit. Based on mammal fauna, a Karpatian age (ca. 17.2–16.4 Ma according to Rögl 1996) has been postulated for the coal from Eibiswald (Mottl 1970). However, according to Rögl's (1996) stratigraphic correlation, the Mammal Zone MN6–5 covers an absolute age span from ca. 17.0–13.0 Ma, which corresponds to nearly the whole Karpatian and Badenian stages. Based on paleogeographic and stratigraphic reasons Gruber et al. (2003) correlated the Eibiswald with the lower coal occurrences exposed in the Hörmsdorf well. Our new $^{40}Ar/^{39}Ar$ ages which have been obtained from two tuff-samples just a few meters in the hanging-wall of this coal horizon, confirm the ideas of Gruber et al. (2003), who argue for a younger, namely Badenian age (16.4–13.0 Ma according to Rögl 1996) for the Eibiswald coal and suggest a minimum age of ca. 15.22 ± 0.17 Ma for the formation of the coal deposits.

As noted above the age of sediments in the area around Pöls is well constrained by biostratigraphic data and regarded as Early Badenian (Kopetzky 1957). Our result of 15.75 ± 0.17 Ma fits perfectly with previously published ages of 16.6 ± 0.6 Ma and 15.1 ± 0.5 Ma, which have been obtained from K-Ar dating on biotite by Balogh et al. (1994).

Conclusions

The new $^{40}Ar/^{39}Ar$ ages presented in this study show the potential to get high-precision ages of tuffs, provided careful sample selection and preparation, although tuffs are mostly altered. Because similar tuffs are widespread not only in the Styrian Basin, but in a number of intramontane basins as well (e.g. Ebner 1981), future work in biostratigraphically well controlled sections could allow further refining of the Paratethyan time-scale calibration. Future work could also allow more precise correlation of the wide marine area of the Pannonian Basin with several small intramontane sedimentary basins, where similar tuffs have been found in mostly terrestrial, lacustrine depositional environments (e.g. Sachsenhofer et al. 2000a,b; Neubauer & Unzog 2003 and references therein).

Acknowledgments: The authors gratefully acknowledge helpful reviews by Dr. J. Lexa, Prof. D. Vass, and one anonymous reviewer.

References

Balogh K., Ebner F. & Ravasz C. 1994: K/Ar-Alter tertiärer Vulkanite der südöstlichen Steiermark und des südlichen Burgenlandes. *Jubiläumsschrift 20 Jahre geologische Zusammenarbeit Österreich – Ungarn Teil 2*, 55–72.

Berggren W.A., Kent D.V., Swisher III C.C. & Aubry M.P. 1995: A revised Cenozoic geochronology and chronostratigraphy. In: Berggren W.A., Kent D.V. & Hardenbol J. (Eds.): Geochronology, time scales and global stratigraphic correlations: A Unified temporal Framework for an Historical Geology. *Soc. Econ. Paleontol. Mineral. Spec. Publ.* 54, 129–212.

Bojar A.-V., Hiden H., Fenninger A. & Neubauer F. 2004: Middle Miocene seasonal temperature changes in the Styrian basin, Austria, as recorded by the isotopic composition of pectinid and brachiopod shells. *Palaeogeogr. Palaeoclimatol. Palaeoecol.* 203, 95–105.

Dobosi G., Schultz-Güttler R., Kurat G. & Kracher A. 1991: Pyroxene chemistry and evolution of alkali basaltic rocks from Burgenland and Styria, Austria. *Mineral. Petrology* 43, 275–292.

Ebner F. 1981: Vulkanische Tuffe im Miozän der Steiermark. *Mitt. Naturwiss. Ver. Steiermark* 111, 39–55.

Ebner F. & Gräf W. 1977: Die Fauna von Weitendorf. *Jber. Landesmus. Joanneum Graz* 1976, N. F. 6, 157–183.

Ebner F. & Sachsenhofer R.F. 1991: Die Entwicklungsgeschichte des Steirischen Tertiärbeckens. *Mitt. Abt. Geol. Paläont. Landesmus. Joanneum* 49, 171–262.

Ebner F., Dunkl I., Mali H. & Sachsenhofer R.F. 2000: Auf dem Weg zu einer Tephrochronologie im Miozän des Alpenostrandes. *Mitt. Gesell. Geol. Bergbaustud. Österr.* 43, 38–39.

Ebner F., Dunkl I., Mali H. & Sachsenhofer R.F. 2002: Stratigraphic evidence of pyroclastic layers in Miocene basins of the Eastern Alps (Austria). Proceedings of the XVII. Congress of the Carpathian-Balkan Geological Association, Bratislava, September 1st–4th 2002. *Geol. Carpathica, Spec. Issue*, CD-ROM, 53, 1–5.

Fenninger A. & Wassermann W. 1982: Clavagellen (Lamellibranchiata) aus den Tonmergeln von Weitendorf (Baden). *Mitt. Naturwiss. Ver. Steiermark* 112, 49–58.

Friebe J.G. 1988: Paläogeographische Überlegungen zu den Leithakalken (Badenien) der Mittelsteirischen Schwelle (Steiermark). *Geol. Paläont. Mitt. Innsbruck* 15, 41–57.

Friebe J.G. 1990: Lithostratigraphische Neugliederung und Sedimentologie der Ablagerungen des Badenium (Miozän) um die Mittelsteirische Schwelle (Steirisches Becken, Österreich). *Jb. Geol. Bundesanst.* 133, 223–257.

Friebe J.G. 1991: Neotektonik an der Mittelsteirischen Schwelle (Österreich): Die "Steirische Phase". *Zbl. Geol. Paläont. Teil I* 1991 H. 1, 41–54.

Fritz I. & Hiden H. 2001: Fossilgrabungen im Steinbruch Retznei (Südsteiermark). Projektmappe für Schulen. *Landesmuseum Joanneum*, Graz, 1–40.

Gross M. 2000: Das Pannonium im Oststeirischen Becken. *Ber. Inst. Geol. Paläont. K.-F.-Univ. Graz* 2, 47–86.

Gruber W., Hermann S., Sachsenhofer R.F. & Stingl K. 2003: Kohlefazies und Sedimentologie der Eibiswalder Bucht (Miozän, Steirisches Becken). *Mitt. Österr. Geol. Gesell.* 93, 15–29.

Hanfland C., Läufer A.L., Nebelsick J.H. & Mossbrugger V. 2004: The Smrekovec Tertiary and related volcanism (Slovenia): sedimentology, geochemistry and tectonic evolution. *Neu. Jb. Geol. Paläont. Abh.* 232, 77–125.

Harangi S., Wilson M. & Tonarini S. 1995: Petrogenesis of Neogene potassic volcanic rocks in the Pannonian Basin. (In): Downes H. & Vaselli O. (Eds.): Neogene and related magmatism in the Carpatho-Pannonian Region. *Acta Vulcanol.* 7, 125–134.

Hauser A. 1951: Ein Vorkommen von Biotitandesit in Retznei bei Ehrenhausen. *Tscherm. Mineral. Petrogr. Mitt.* 2, 3, 157–165.

Kolmer H. 1980: Das Rb-Sr-Alter oststeirischer Vulkanite. *Mitt. Naturwiss. Ver. Steiermark* 110, 23–26.

Krainer B. 1987: Sedimentation und Shoshonit von Weitendorf, Badenien, Steirisches Becken. *Mitt. Österr. Geol. Gesell.* 80, 143–156.

Kopetzky G. 1957: Das Miozän zwischen Kainach und Laßnitz in Südweststeiermark. *Mitt. Mus. Bergbau, Geol. Techn.* 18, 1–112.

Lippolt J., Baranyi I. & Todt W. 1975: Das Kalium-Argon-Alter des Basaltes vom Lavant-Tal in Kärnten. *Der Aufschluss* 26, 238–242.

Ludwig K.R. 2001: ISOPLOT/EX v. 2.49 — A geochronological toolkit for Microsoft Excel. *Berkeley Geochronol. Cent. Spec. Publ.* 1a, 1–49.

McDougall I. & Harrison M.T. 1999: Geochronology and thermochronology by the $^{40}Ar/^{39}Ar$ method. 2nd Ed. *Oxford University Press,* New York–Oxford, 1–269.

Mottl M. 1970: Die jungtertiären Säugetierfaunen der Steiermark, Südostösterreich. *Mitt. Mus. Bergbau Geol. Techn. Landesmus. Joanneum* 31, 12–69.

Neubauer F. & Unzog W. 2003: Halfgraben formation within an extruding wedge: the Neogene Waldheimat basin in the Eastern Alps. *Neu. Jb. Geol. Paläont. Abh.* 230, 133–154.

Piller W.E., Egger H., Erhart C., Gross M., Harzhauser M., Hubmann B., van Husen D., Krenmayr H.-G., Krystyn L., Lein R., Lukeneder A., Mandl G., Rögl F., Roetzel R., Rupp C., Schnabel W., Schönlaub H.P., Summesberger H. & Wagreich M. 2004: Die Stratigraphische Tabelle von Österreich 2004 (Sedimentäre Schichtfolge). Österreichische Stratigraphische Kommission. *Österr. Akademie der Wissenschaften,* Wien.

Rögl F. 1996: Stratigraphic correlation of the Paratethys Oligocene and Miocene. *Mitt. Gesell. Geol. Bergbaustud. Österr.* 41, 65–73.

Rögl F. 1998: Paleogeographic considerations for Mediterranean and Paratethys seaways (Oligocene to Miocene). *Ann. Naturhist. Mus. Wien* 99A, 279–310.

Rögl F. 1999: Mediterranean and Paratethys. Facts and hypotheses of an Oligocene to Miocene Paleogeography (Short Overview). *Geol. Carpathica* 50, 4, 339–349.

Rögl F. 2001: Mid-Miocene Circum Mediterranean paleogeography, environmental and ecosystem dynamics of the Eurasian Neogene. Stratigraphy and paleogeography workshop in Graz. *Ber. Inst. Geol. Paläont. K.-F.-Univ. Graz*, 49–59.

Sachsenhofer R.F., Dunkl I., Hasenhüttl C. & Jelen B. 1998: Miocene thermal history of the southwstern margin of the Styrain Basin: vitrinite reflectance and fission-track data from the Pohorje/Kozjak area (Slovenia). *Tectonophysics* 297, 17–29.

Sachsenhofer R.F., Kogler A., Polsny H., Strauss P. & Wagreich M. 2000a: The Neogene Fohnsdorf Basin: basin formation and basin inversion during lateral extrusion in the Eastern Alps (Austria). *Int. J. Earth Sci.* 89, 415–430.

Sachsenhofer R.F., Strauss P., Wagreich M., Abart R., Decker K., Goldbrunner J.E., Gruber W., Kriegl C. & Spötl C. 2000b: Das miozäne Fohnsdorfer Becken — eine Übersicht. *Mitt. Gesell. Geol. Bergbaustud. Österr.* 44, 173–190.

Steiger R.H. & Jäger E. 1977: Subcommission on geochronology: Convention on the use of decay constants in geo- and cosmochronology. *Earth Planet. Sci. Lett.* 36, 359–362.

Steininger F.F. 1999: Chronostratigraphy, geochronology and biochronology of the "European Land Mammal Mega-Zones" (ELMMZ) and the Miocene "Mammal-Zones" (MN-Zones). In: Rössner G.E. & Heissig K. (Eds.): The Miocene land mammals of Europe. *Dr. Friedrich Pfeil,* München, 9–24.

Steininger F.F. & Bagdasarjan G.P. 1977: Neue radiometrische Alter mittelmiozäner Vulkanite der Steiermark (Österreich), ihre biostratigraphische Korrelation und ihre möglliche Stellung innerhalb der paläomagnetischen Zeitskala. *Verh. Geol. Bundesanst.* 1977, H. 2, 85–99.

Steininger F.F. & Wessely G. 2000: From the Tethyan Ocean to the Paratethys Sea: Oligocene to Neogene stratigraphy, paleogeography and paleobiogeography of the circum-Mediterranean region and the Oligocene to Neogene Basin evolution in Austria. *Mitt. Österr. Geol. Gesell.* 92, 95–116.

Steininger F.F., Berggren W.A., Kent D.V., Bernor R.L., Sen S. & Agusti J. 1996: Circum Mediterranean Neogene (Miocene and Pliocene) marine-continental chronologic correlations of European mammal units and zones. In: Bernor R.L., Fahlbusch V. & Rietschel S. (Eds.): Later Neogene European biotic evolution and stratigraphic correlation. *Columbia University Press*, New York, 7–46.

Steininger F.F., Daxner-Höck G., Haas M., Kovar-Eder J., Mauritsch H.J., Meller B. & Scholger R.M. 1998: Stratigraphy of the „Basin Fill" in the Early Miocene lignite opencast mine Oberdorf (N Voitsberg, Styria, Austria). *Jb. Geol. Bundesanst.* 140, 397–402.

Vass D. & Balogh K. 1989: The period of main and late Alpine molasses. *Z. Geol. Wiss.* 17, 849–858.

Wijbrans J.R., Pringle M.S., Koopers A.A.P. & Schveers R. 1995: Argon geochronology of small samples using the Vulkaan argon laserprobe. *Proc. Kon. Nederl. Akad. Wetensch.* 98, 2, 185–218.

York D. 1969: Least-squares fitting of a straight line with correlated errors. *Earth Planet. Sci. Lett.* 5, 320–324.